High-throughput screening reveals new glutaminase inhibitor molecules

Renna K. E. Costa [1,2]†, Camila Rodrigues†[3], Jean C. H. Campos[1]†, Luciana Paradela [1,2]†, Marilia M. Dias [1], Bianca Novaes da Silva[1], Cyro von Zuben de Valega Negrao[1,2], Kaliandra de Almeida Gonçalves[1], Carolline F. R. Ascenção [1,2], Douglas Adamoski [1,2], Gustavo Fernando Mercaldi[1], Alliny C. S. Bastos[1], Fernanda A. H. Batista[1], Ana Carolina Figueira[1], Artur T. Cordeiro[1], Andre L. B. Ambrosio[1], Rafael V. C. Guido[3]*†, Sandra M. G. Dias[1]*†

Supplementary Information

Supplementary Figure 1

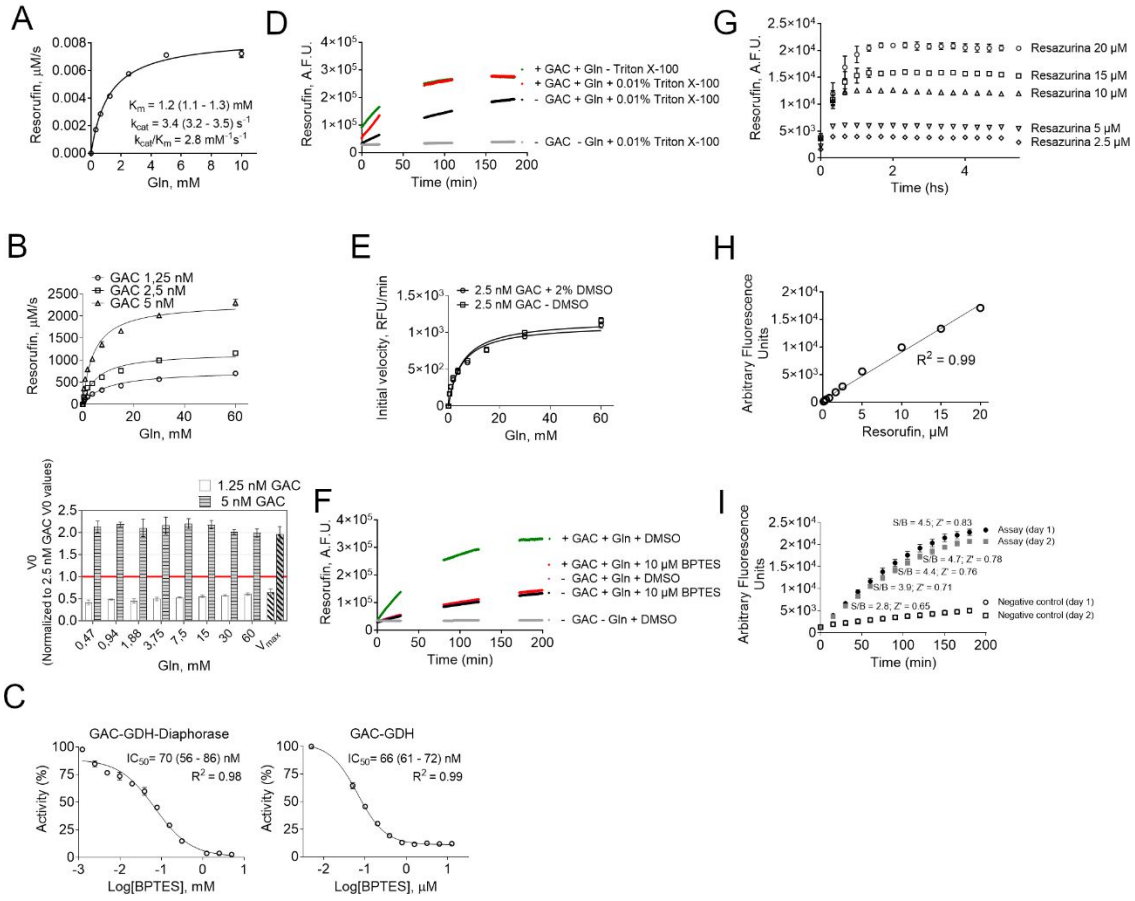

Supplementary Figure S1. Assay optimization. *A*, Michaelis-Menten of the GAC-GDH-Diaphorase fluorescent coupled assay. Obtained K_m, k_{cat} and k_{cat}/K_m for 2.5 nM of enzyme are very close to the same parameters measured for GAC in a GAC-GDH absorbance assay previously published (41) (see table for comparison). *B*, Above, Michaelis-Menten of the GAC-GDH-Diaphorase fluorescent coupled assay using 1,25 nM and 5 nM; below, the ratio between V0 measured for each glutamine concentration (and Vmax) when using 1,25 nM GAC over 2,5 nM GAC (white bars) or 5 nM GAC over 2,5 nM GAC (gray bars), showing the values are proportional to the GAC concentration. The proportionality proves the reaction is driven by GAC. *C*, comparing the IC_{50} of BPTES over the GAC-GDH-Diaphorase fluorescent coupled assay and the GAC-GDH absorbance assay. *D*, Measured RFU of the GAC-GDH-Diaphorase fluorescent coupled assay over time showing that 0.01% Triton X-100 does not affect measurement. *E*, Michaelis-Menten of the GAC-GDH-Diaphorase fluorescent coupled assay showing that 2% DMSO does not affect the curve qualitatively. *F*, Measured RFU of the GAC-GDH-Diaphorase fluorescent coupled assay in different conditions over 200 minutes showing

that either GAC removal (-GAC +Gln + 2% DMSO) or BPTES 10 µM (+GAC + Gln + 10 µM BPTES) treatment gives equivalent measurements. *G*, Measured RFU of the GAC-GDH-Diaphorase fluorescent coupled assay over time showing that 20 µM resorufin gives the highest signal and best S/N (values not shown). *H*, RFU obtained for different amounts (0 to 20 µM) of the fluorescent product, resorufin, showing the dynamic range of the reaction. *I*, Reproducibility of the GAC-GDH-Diaphorase fluorescent coupled assay over two consecutive days. Z' and S/B for each data point of Assay (day 1).

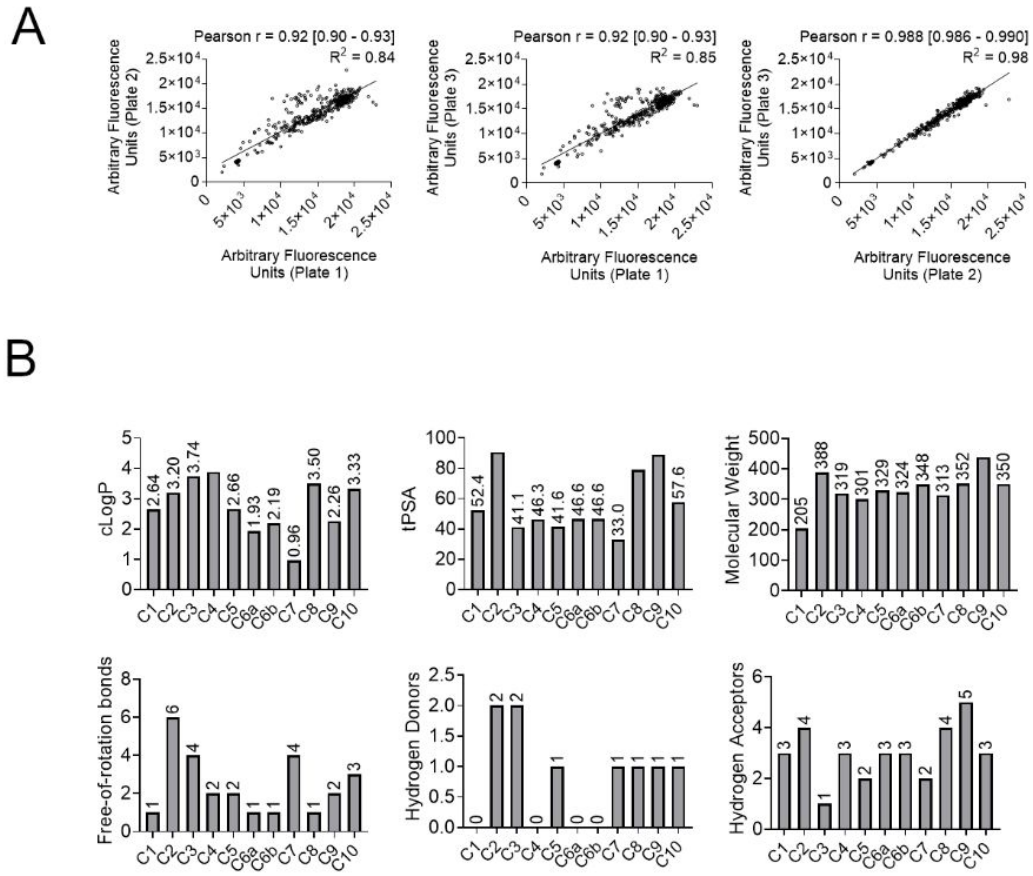

Supplementary Figure S2. *A*, Confirmation assay of 320 hits was performed in triplicate after cherry-picking. Correlation between plate 1 and 2 (on the left), plates 1 and 3 (in between) and plates 2 and 3 (on the right). Pearson correlation r and R^2 values are shown above each graph. *B*, cLogP, topological polar superficial area (tPSA), Molecular Weight, number of free-of-rotation bonds, number of hydrogen bonds donors and acceptors graphs of the 11 re-supplied compounds.

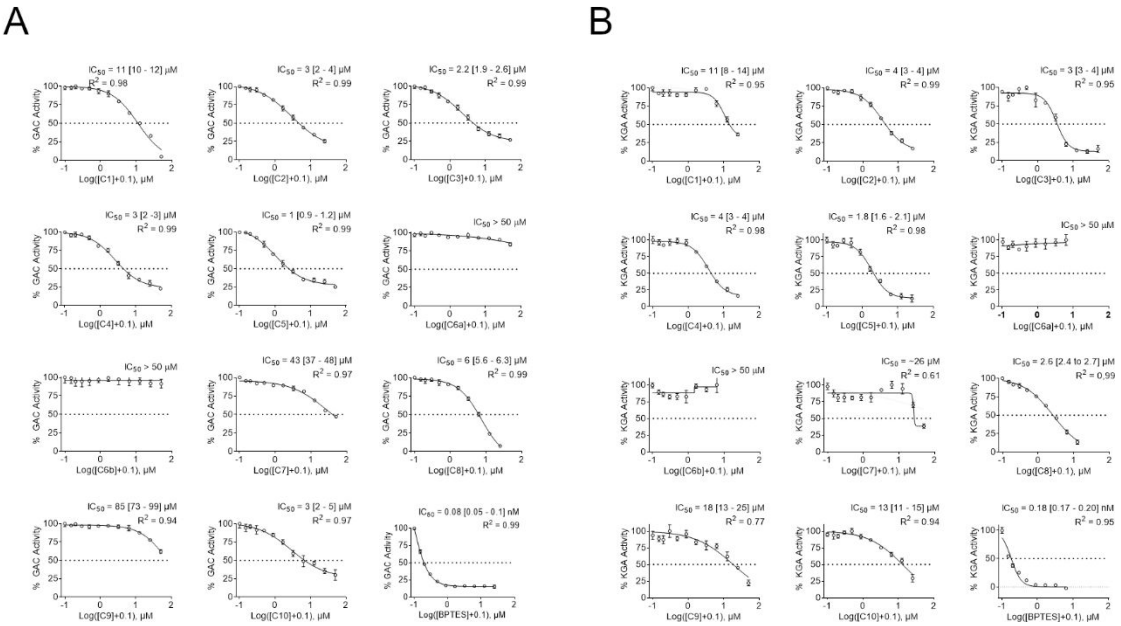

Supplementary Figure S3. *A*, curves of C1-C10 on the GAC (A) or KGA (B) enzymatic activity. Values within the brackets represents an interval confidence of 95% (CI 95%).

Supplementary Figure 4

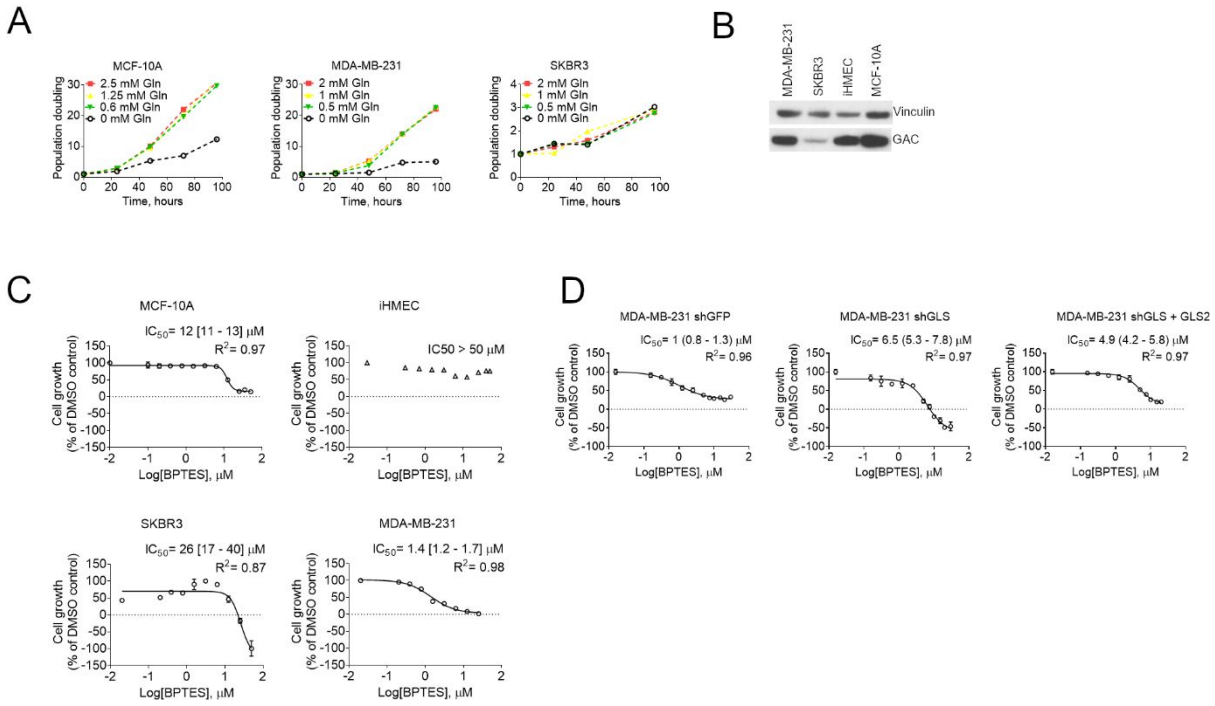

Supplementary Figure S4. Glutamine-deprivation and BPTES effect on cell growth. *A*, Growth response assay of MDA-MB-231, a TNBC cell line, SKBR3, a non-TNBC cell line and the non-tumorigenic MCF-10A cell line to different concentrations of glutamine in the media. *B*, Western blot showing the GLS levels in the cell lines. Growth dose-response assay of BPTES over MDA-MB-231, SKBR3, MCF-10A and hTert-immortalized iHMEC (*C*) and MDA-MB-231 shGFP, shGLS and shGLS expressing GLS2 ectopically (*D*). On (*C*, *D*), the data was normalized and 0% was set as the number of seeded cells and 100% as the highest number of cells. Doses bellow the dashed lines indicate the concentrations that lead to cell death (final number of cells after 48 hours is smaller than the number of seeded cells). IC_{50} [95% CI] and R^2 of the adjusted sigmoidal curve are displayed. Graphics in *A*, *C*-*D*, each bar represents the mean ± SD of n = 4 replicates.

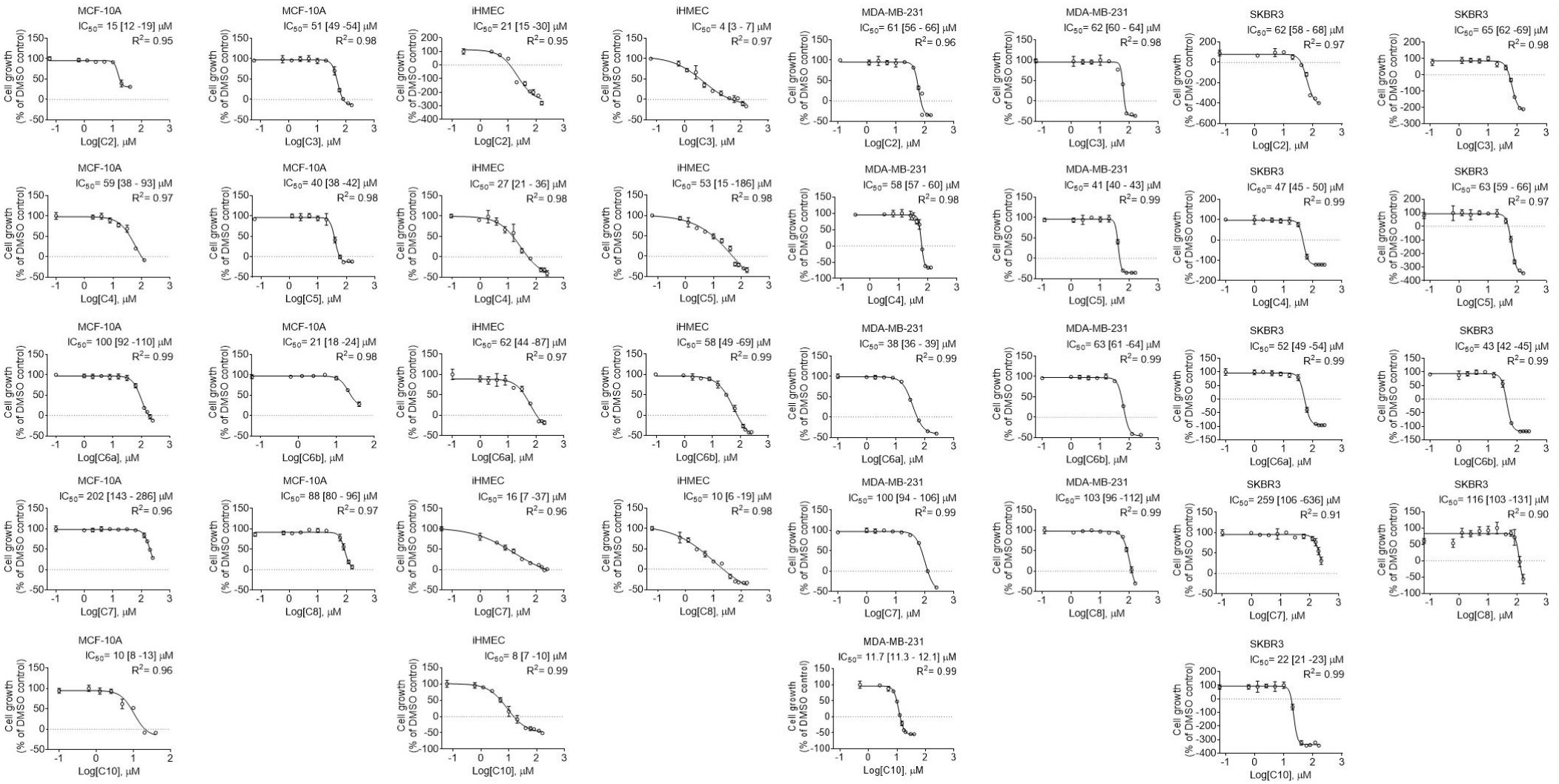
MCF-10A
IC50= 15 [12 -19] µM
R2= 0.95
Cell growth (% of DMSO control)
Log[C2], µM
MCF-10A
IC50= 51 [49 -54] µM
R2= 0.98
Log[C3], µM
iHMEC
IC50= 21 [15 -30] µM
R2= 0.95
Log[C2], µM
iHMEC
IC50= 4 [3 - 7] µM
R2= 0.97
Log[C3], µM
MDA-MB-231
IC50= 61 [56 - 66] µM
R2= 0.96
Log[C2], µM
MDA-MB-231
IC50= 62 [60 - 64] µM
R2= 0.98
Log[C3], µM
SKBR3
IC50= 62 [58 - 68] µM
R2= 0.97
Log[C2], µM
SKBR3
IC50= 65 [62 -69] µM
R2= 0.98
Log[C3], µM
MCF-10A
IC50= 59 [38 - 93] µM
R2= 0.97
Log[C4], µM
MCF-10A
IC50= 40 [38 -42] µM
R2= 0.98
Log[C5], µM
iHMEC
IC50= 27 [21 - 36] µM
R2= 0.98
Log[C4], µM
iHMEC
IC50= 53 [15 -186] µM
R2= 0.98
Log[C5], µM
MDA-MB-231
IC50= 58 [57 - 60] µM
R2= 0.98
Log[C4], µM
MDA-MB-231
IC50= 41 [40 - 43] µM
R2= 0.99
Log[C5], µM
SKBR3
IC50= 47 [45 - 50] µM
R2= 0.99
Log[C4], µM
SKBR3
IC50= 63 [59 - 66] µM
R2= 0.97
Log[C5], µM
MCF-10A
IC50= 100 [92 -110] µM
R2= 0.99
Log[C6a], µM
MCF-10A
IC50= 21 [18 -24] µM
R2= 0.98
Log[C6b], µM
iHMEC
IC50= 62 [44 -87] µM
R2= 0.97
Log[C6a], µM
iHMEC
IC50= 58 [49 -69] µM
R2= 0.99
Log[C6b], µM
MDA-MB-231
IC50= 38 [36 - 39] µM
R2= 0.99
Log[C6a], µM
MDA-MB-231
IC50= 63 [61 -64] µM
R2= 0.99
Log[C6b], µM
SKBR3
IC50= 52 [49 -54] µM
R2= 0.99
Log[C6a], µM
SKBR3
IC50= 43 [42 -45] µM
R2= 0.99
Log[C6b], µM
MCF-10A
IC50= 202 [143 - 286] µM
R2= 0.96
Log[C7], µM
MCF-10A
IC50= 88 [80 - 96] µM
R2= 0.97
Log[C8], µM
iHMEC
IC50= 16 [7 -37] µM
R2= 0.96
Log[C7], µM
iHMEC
IC50= 10 [6 -19] µM
R2= 0.98
Log[C8], µM
MDA-MB-231
IC50= 100 [94 - 106] µM
R2= 0.99
Log[C7], µM
MDA-MB-231
IC50= 103 [96 -112] µM
R2= 0.99
Log[C8], µM
SKBR3
IC50= 259 [106 -636] µM
R2= 0.91
Log[C7], µM
SKBR3
IC50= 116 [103 -131] µM
R2= 0.90
Log[C8], µM
MCF-10A
IC50= 10 [8 -13] µM
R2= 0.96
Log[C10], µM
iHMEC
IC50= 8 [7 -10] µM
R2= 0.99
Log[C10], µM
MDA-MB-231
IC50= 11.7 [11.3 - 12.1] µM
R2= 0.99
Log[C10], µM
SKBR3
IC50= 22 [21 -23] µM
R2= 0.99
Log[C10], µM

Supplementary Figure S5. IC_{50} curves of C2-C8 and C10 on the MCF-10A, iHMEC, MDA-MB-231 and SKBR3 cell lines growth. Values within the brackets represents an interval confidence of 95% (CI 95%).

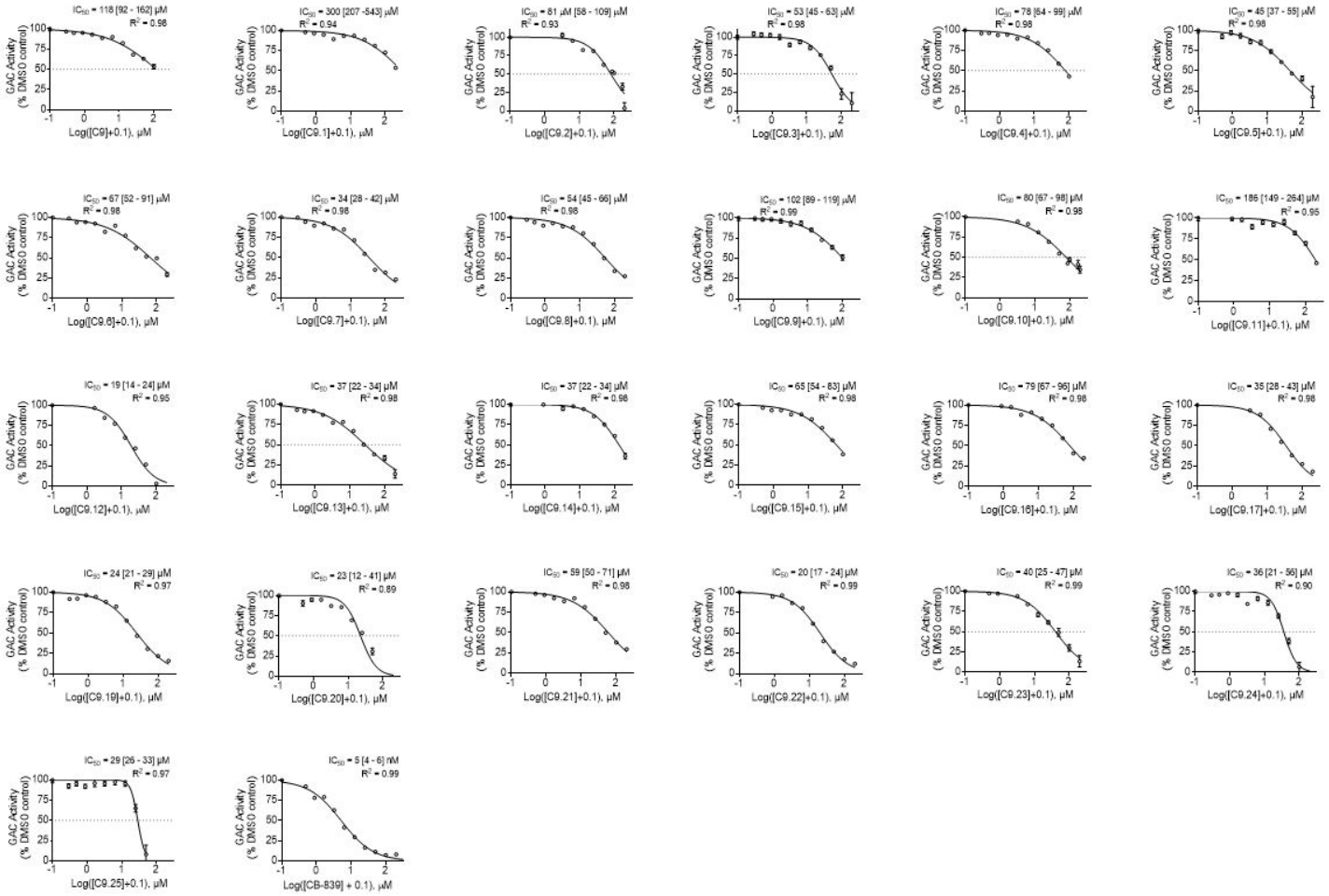

Supplementary Figure S6. IC_{50} curves of C9 analogues on the GAC enzymatic activity. Values within the brackets represents an interval confidence of 95% (CI 95%).

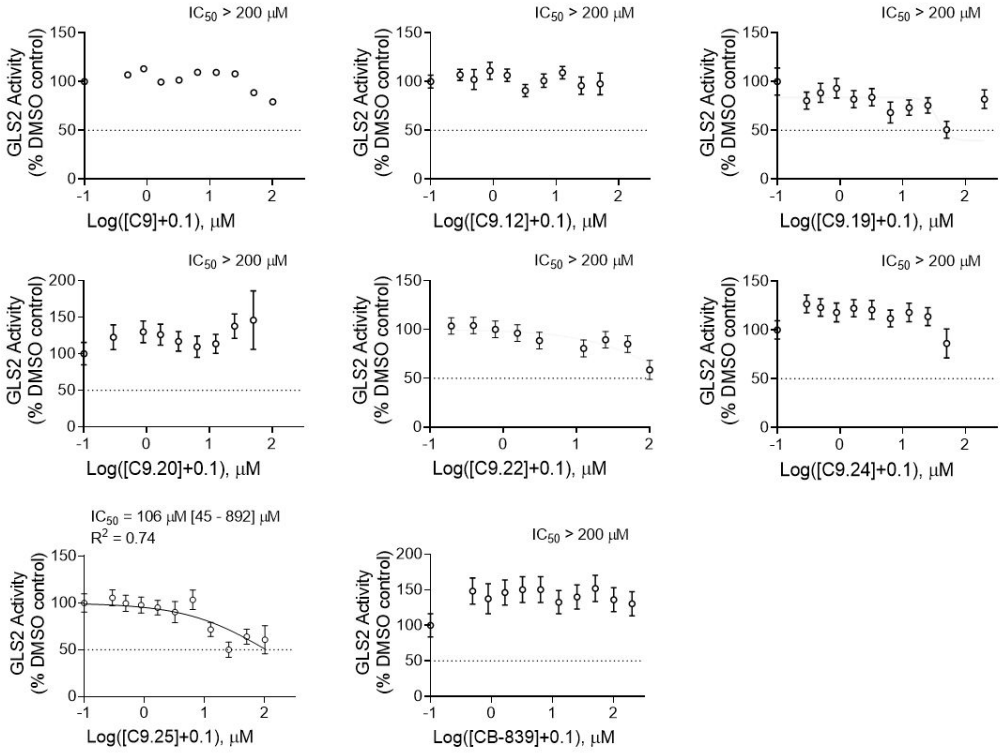

Supplementary Figure S7. IC_{50} curves of selected C9 analogues on the GLS2 enzymatic activity. Values within the brackets represents an interval confidence of 95% (CI 95%).

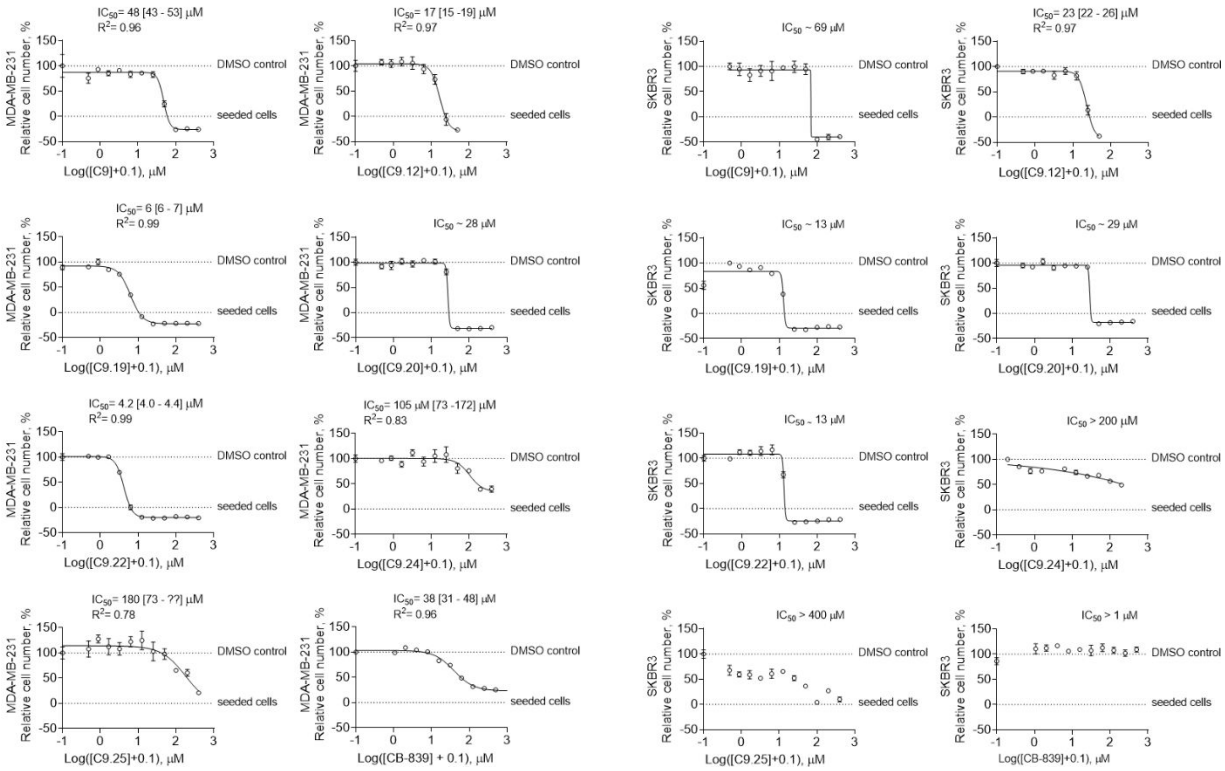

Supplementary Figure S8. IC_{50} curves of selected C9 analogues on the MDA-MB-231 (on the left) and SKBR3 (on the right) cell lines growth. Values within the brackets represents an interval confidence of 95% (CI 95%).

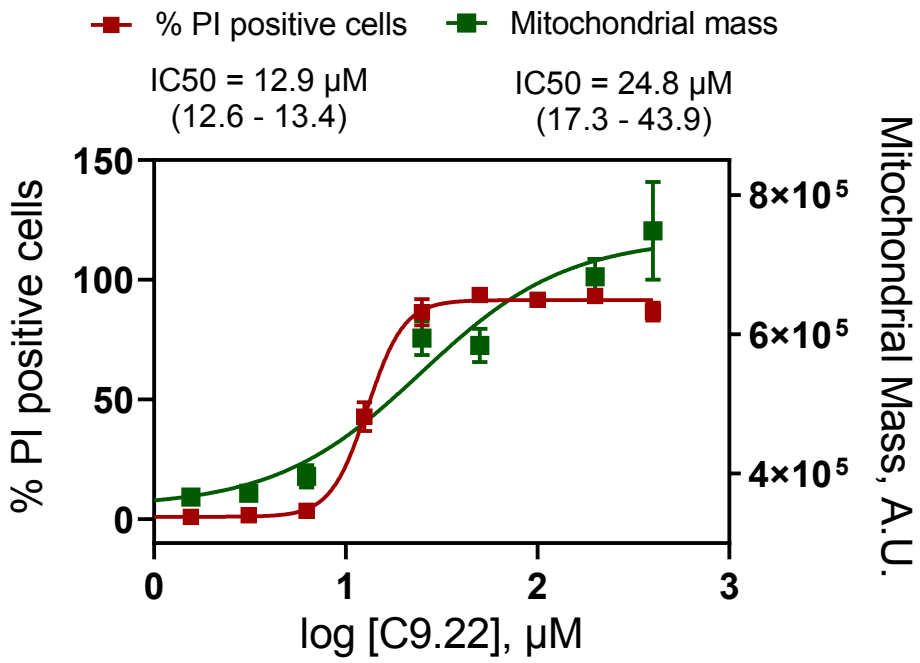

Supplementary Figure 9. IC_{50} curves of C9.22 on the MDA-MB-231 cell line for necrosis (propidium iodide, PI) and mitochondrial mass stainning (Mitotracker Deep Red; cytotoxicity marker). Values within the brackets represents an interval confidence of 95%.

Supplementary Table S1 - Excel file with 6 spreadsheets containing raw and processed HTS data; Provided as a separated file.

Supplementary Table S2 – The final 100 compounds hit list.

Compound ressuplied	Compoud # (100 final hits)	Chembridge number	% inhibition GAC retest average	% inhibition GDH/Diaphorase	% inhibition GAC retest average - % inhibition GDH	Cluster #
	1	5251606	105.8	17.8	88.0	non-clustered
	2	5455995	88.7	0.0	88.7	non-clustered
	3	7983133	88.6	24.7	63.9	non-clustered
	4	9109040	87.0	3.7	83.3	G4
	5	5266583	85.8	2.3	83.5	non-clustered
	6	6985461	79.7	17.1	62.6	non-clustered
(C1)	7	7992402	73.4	0.0	73.4	non-clustered
(C2)	8	9155049	72.9	2.4	70.5	G11
	9	7975549	72.3	13.9	58.4	non-clustered
	10	5917156	72.2	11.0	61.2	G17
(C3)	11	7956101	69.2	0.0	69.2	non-clustered
(C4)	12	9125354	69.2	0.0	69.2	G2
(C5)	13	7952342	68.5	0.0	68.5	G7
(C6a)	14	6744277	60.2	0.0	60.2	G12
(C7)	15	5354303	60.2	0.0	60.2	G5
(C8)	16	7962214	58.3	0.0	58.3	non-clustered
(C6b)	17	5603967	57.3	0.0	57.3	G12
	18	7992232	57.2	0.0	57.2	G15
	19	9038938	57.0	0.0	57.0	non-clustered
	20	9001794	56.8	0.2	56.6	non-clustered
	21	5919129	56.7	8.2	48.4	G17
	22	5331342	54.6	11.3	43.3	G6
	23	7832691	53.7	0.0	53.7	G15
	24	7874229	52.8	5.0	47.7	non-clustered
	25	5141313	51.7	0.0	51.7	non-clustered
	26	6573489	51.7	12.4	39.3	non-clustered
	27	9074873	51.7	13.3	38.4	G8
	28	7954758	51.2	0.0	51.2	G3

	29	9007772	51.0	0.0	51.0	non-clustered
	30	9082772	50.5	0.0	50.5	G13
(C9)	31	9007737	50.0	0.0	50.0	non-clustered
	32	5346214	49.3	0.0	49.3	G5
(C10)	33	7951061	48.3	0.0	48.3	G12
	34	9064772	47.3	0.0	47.3	G14
	35	7943337	46.6	0.7	45.9	G16
	36	5211912	46.4	13.3	33.2	non-clustered
	37	9123924	46.4	0.0	46.4	non-clustered
	38	9077494	46.4	1.2	45.1	G13
	39	6373017	46.3	0.0	46.3	non-clustered
	40	9125395	46.1	0.0	46.1	G2
	41	5478253	45.9	0.0	45.9	non-clustered
	42	9139619	45.6	0.0	45.6	non-clustered
	43	5621638	45.2	0.0	45.2	G12
	44	5319283	42.3	14.5	27.8	non-clustered
	45	7893819	41.9	0.0	41.9	G13
	46	7797911	41.7	2.7	39.1	non-clustered
	47	7969373	41.7	12.3	29.4	non-clustered
	48	7615470	41.6	1.4	40.1	non-clustered
	49	7946808	40.8	12.2	28.6	G11
	50	7690736	40.7	11.4	29.2	non-clustered
	51	5348920	40.5	0.0	40.5	G5
	52	7987960	40.3	0.0	40.3	non-clustered
	53	9064882	40.1	0.0	40.1	G15
	54	9102535	39.4	0.0	39.4	G4
	55	7970522	38.8	0.0	38.8	G7
	56	7953673	38.8	6.0	32.8	non-clustered
	57	7745039	38.8	5.4	33.5	G8
	58	7950985	38.7	0.0	38.7	non-clustered
	59	9108360	38.6	2.8	35.8	G13
	60	9014421	38.1	10.3	27.8	G10
	61	9153561	37.8	0.2	37.6	non-clustered
	62	6946489	37.2	7.2	29.9	non-clustered
	63	5350946	37.1	0.0	37.1	G5
	64	7257347	36.7	0.0	36.7	non-clustered

	65	9010720	36.7	0.0	36.7	G12
	66	5857415	36.7	0.0	36.7	non-clustered
	67	9106880	36.5	0.0	36.5	G4
	68	9109696	36.4	5.1	31.4	non-clustered
	69	9007162	35.8	1.6	34.2	non-clustered
	70	7967624	34.9	0.0	34.9	G3
	71	9082761	34.8	0.0	34.8	G14
	72	7967883	34.6	0.0	34.6	non-clustered
	73	9001315	34.5	0.0	34.5	G11
	74	7991342	34.0	0.0	34.0	non-clustered
	75	9004059	33.8	0.0	33.8	G16
	76	9062228	32.8	0.0	32.8	non-clustered
	77	9101689	32.5	0.0	32.5	non-clustered
	78	7931360	32.1	0.0	32.1	G6
	79	7998861	31.9	5.7	26.2	non-clustered
	80	9096238	30.1	0.0	30.1	non-clustered
	81	9109980	29.6	0.0	29.6	G4
	82	7644288	29.4	0.0	29.4	G10
	83	7962071	29.2	0.2	29.0	non-clustered
	84	9078534	28.9	0.0	28.9	non-clustered
	85	9155265	28.7	0.0	28.7	non-clustered
	86	7569611	28.6	0.0	28.6	non-clustered
	87	7934875	28.5	0.0	28.5	non-clustered
	88	9063041	28.1	0.0	28.1	G9
	89	5924787	27.7	0.8	26.9	G1
	90	5930037	26.5	0.0	26.5	G1
	91	7625548	26.2	0.0	26.2	non-clustered
	92	7980582	25.5	0.0	25.5	non-clustered
	93	9059254	24.6	0.0	24.6	G9
	94	7938972	24.1	0.0	24.1	non-clustered
	95	7945021	24.0	0.0	24.0	non-clustered
	96	7997020	23.6	0.0	23.6	G12
	97	9102488	23.1	0.0	23.1	G4
	98	5373315	20.3	0.0	20.3	non-clustered
	99	5612286	19.8	0.0	19.8	G12
	100	9120786	19.4	0.0	19.4	non-clustered

Supplementary Table S3 - Drug-like properties calculated by the OpenBabel.

	Druglikeness	Mutagenic	Tumorigenic	Reproductive Effective	Irritant
C1	-4.9666	none	none	none	none
C2	2.5939	none	none	none	none
C3	2.6252	none	none	none	none
C4	4.0452	none	none	none	none
C5	0.7881	none	high	low	high
C6a	2.4671	none	none	high	low
C7	-1.182	none	none	none	none
C8	4.0127	high	high	high	low
C6b	0.5554	none	none	high	none
C9	2.0762	none	none	none	none
C10	4.3483	none	none	none	none
968	-2.34	none	none	none	none

BPTES	3.9388	none	none	none	none
CB-839	-9.1868	none	none	none	none

Supplementary Table S4- *In silico* safety. ADME and physicochemical profile of the 11 resupplied compounds.

	Drug Safety Profiling								ADME Profiling					PhysChem Profiling								
ID	P-gp Substrates	CYP1A2 Inhibitor	CYP2C9 Inhibitor	CYP2C19 Inhibitor	CYP2D6 Inhibitor	CYP3A4 Inhibitor	Ames	hERG	Caco-2	PPB	CNS	HIA	Metabolic Stability	LogP	MW	H-Donors	H-Acceptors	Rot. Bonds	Rings	Lipinski	Lead-like	Solubility
968	Undefined	Undefined	Undefined	Undefined	Undefined	Undefined	Undefined	Undefined	Highly permeable	Extensively bound	Non-penetrant	Highly absorbed	Undefined	Very lipophilic	Moderate	Good	Good	Good	Bad	Moderate	Bad	Highly insoluble
BPTES	Undefined	Undefined	Undefined	Undefined	Undefined	Undefined	Undefined	Undefined	Highly permeable	Undefined	Non-penetrant	Highly absorbed	Undefined	Optimal	Bad	Good	Good	Bad	Good	Moderate	Moderate	Highly insoluble
CB-839	Undefined	Undefined	Undefined	Undefined	Undefined	Undefined	Undefined	Undefined	Highly permeable	Undefined	Non-penetrant	Highly absorbed	Undefined	Optimal	Bad	Good	Good	Bad	Good	Moderate	Bad	Highly insoluble
C1	Undefined	Undefined	Undefined	Undefined	Undefined	Non-inhibitor	Undefined	Undefined	Highly permeable	Strongly bound	Penetrant	Highly absorbed	Undefined	Optimal	Good	Good	Good	Good	Good	Good	Good	Insoluble
C2	Undefined	Undefined	Undefined	Undefined	Undefined	Undefined	Undefined	Undefined	Highly permeable	Undefined	Penetrant	Highly absorbed	Undefined	Optimal	Good	Good	Good	Good	Good	Good	Good	Soluble
C3	Undefined	Undefined	Undefined	Undefined	Undefined	Undefined	Undefined	Undefined	Highly permeable	Extensively bound	Penetrant	Highly absorbed	Undefined	Optimal	Good	Good	Good	Good	Good	Good	Good	Highly insoluble
C4	Undefined	Undefined	Undefined	Undefined	Undefined	Undefined	Undefined	Undefined	Highly permeable	Strongly bound	Penetrant	Highly absorbed	Undefined	Optimal	Good	Good	Good	Good	Good	Good	Good	Soluble
C5	Undefined	Undefined	Undefined	Undefined	Undefined	Undefined	Undefined	Undefined	Highly permeable	Moderately bound	Penetrant	Highly absorbed	Undefined	Optimal	Good	Good	Good	Good	Good	Good	Good	Insoluble
C6a	Undefined	Undefined	Undefined	Undefined	Non-inhibitor	Undefined	Undefined	Undefined	Highly permeable	Strongly bound	Penetrant	Highly absorbed	Undefined	Optimal	Good	Good	Good	Good	Good	Good	Good	Highly insoluble
C7	Undefined	Undefined	Undefined	Undefined	Undefined	Undefined	Undefined	Undefined	Moderately permeable	Weakly bound	Weak penetrant	Poorly absorbed	Undefined	Very hydrophilic	Good	Good	Good	Good	Good	Moderate	Moderate	
C8	Undefined	Undefined	Undefined	Undefined	Non-inhibitor	Undefined	Undefined	Undefined	Highly permeable	Extensively bound	Penetrant	Highly absorbed	Undefined	Optimal	Good	Good	Good	Good	Good	Good	Good	Highly insoluble
C6b	Undefined	Undefined	Undefined	Undefined	Undefined	Undefined	Undefined	Undefined	Highly permeable	Moderately bound	Penetrant	Highly absorbed	Undefined	Optimal	Good	Good	Good	Good	Good	Good	Good	Insoluble

C9	Undefined	Undefined	Undefined	Undefined	Undefined	Undefined	Undefined	Undefined	Highly permeable	Moderately bound	Penetrant	Highly absorbed	Undefined	Optimal	Good	Good	Good	Good	Good	Good	Good	Highly insoluble
C10	Undefined	Undefined	Undefined	Undefined	Undefined	Undefined	Undefined	Undefined	Highly permeable	Extensively bound	Penetrant	Highly absorbed	Undefined	Optimal	Good	Good	Good	Good	Good	Good	Good	Insoluble